Comparative analysis of the distribution and morphology of tactile hairs on the wing membrane of four bat species

S. J. Sterbing* and C. F. Moss

Department of Psychology, Institute for Systems Research, University of Maryland, College Park, MD 20742, USA (SJS, CFM)
Present address of SJS and CFM: Department of Psychological and Brain Sciences, Johns Hopkins University, 3400 N. Charles St., Ames Hall, Baltimore, MD 21210, USA

* Correspondent: ssterbi1@jhu.edu

The bat wing is a highly adaptive airfoil that enables demanding flight maneuvers that are performed with robustness under turbulent conditions, and stability at slow flight speeds. The bat wing is covered with microscopically small, tactile hairs that have been shown to be involved in sensing air flow for improved flight maneuverability in 2 bat species, the frugivorous–nectarivorous *Carollia perspicillata* and the insectivorous *Eptesicus fuscus.* Here, we provide comparative data on the anatomy of these hairs and their distribution on the wing surface in 4 species of bats (*C. perspicillata*, *Desmodus rotundus*, *E. fuscus*, and *Rousettus aegyptiacus*), based on scanning electron microscopy analyses. Hairs were found on both the dorsal and ventral surfaces of the wing in all species, including the bony structures. They were generally sparsely distributed (1–3 hairs/mm^2) and often found arranged in single file along elastin bands that extend through the wing membrane. Fringes of hairs also were found at the leading edge of the propatagium. The hairs were strongly tapered in all species. Their length varied from 0.08 mm (*E. fuscus*) to 3 mm (*R. aegyptiacus*). Hair length correlated positively with the body mass and wing loading value of each species, but not with aspect ratio, flight speed, or diet. We conclude that the hairs are spaced so that viscous coupling is negligible, at least for single-file hairs, and that they are scaled to the boundary layer of airflow limited to the first few millimeters close to the wing surface.

Key words: bat, biological systems, scanning electron microscopy, tactile sensors

Bats are the second-largest group of mammals, with over 1,300 species, and they are the only mammals with powered flight. The bat wing is covered with microscopically small, tactile hairs that have been shown to be involved in sensing airflow for improved flight maneuverability in 2 bat species, the frugivorous and nectarivorous *Carollia perspicillata* and the insectivorous *Eptesicus fuscus* (Sterbing-D'Angelo et al. 2011). The bat's wing membrane is unusually thin and is lacking glabrous skin that is typically found on the ventral surface of the hands of other mammals. Hence, wing hairs are found on both the dorsal and ventral sides of the hand.

Bats live in a variety of habitats, and their flight requirements are diverse. With the goal of characterizing wing hairs in bat species with diverse flight behaviors, we studied the hairs on the wing membrane of 4 species: the insectivorous big brown bat (*E. fuscus*, Vespertilionidae), the frugivorous and nectarivorous short-tailed fruit bat (*C. perspicillata*, Phyllostomidae), the sanguivorous vampire bat (*Desmodus*

rotundus, Phyllostomidae), and the frugivorous Egyptian fruit bat (*Rousettus aegyptiacus*, Pteropodidae). These species exhibit different flight specializations related to their particular diets and habitats and exhibit a wide range of body mass and wing loading, i.e., the quotient of body mass and wing area.

The bat wing is an adaptive airfoil that enables flight maneuvers that are performed with robustness under turbulent conditions, and stability at slow flight speeds. Particle-imaging velocimetry studies revealed that bat flight generates complex aerodynamic tracks with wake vortices, i.e., areas of turbulent, reverse airflow, mainly along the dorsal leading edge and trailing edges of the wing (Muijres et al. 2008). Neurons in the somatosensory cortex of *E. fuscus* show mostly directional responses to airflow, preferring reverse airflow as caused by the dorsal leading edge vortex during slow flight (Sterbing-D'Angelo et al. 2011; Muijres et al. 2014; Sterbing-D'Angelo et al. 2017). Hence, we predicted that the wing-hair morphology and

1

distribution of hairs would reflect species differences such as body mass, wing span, aspect ratio, wing loading, diet, or flight speed.

MATERIALS AND METHODS

Animals.—All tissue used in this study was collected from freshly euthanized bats with intact wings. *Eptesicus fuscus* were wild-caught in Maryland under a permit from the Maryland Department of Natural Resources following the Guidelines of the American Society of Mammalogists for the use of wild mammals in research (Sikes et al. 2016). *Carollia perspicillata*, native to Central America, was imported from the Montréal Biodôme, Canada. *Desmodus rotundus* wings were provided by the Wilkinson Laboratory at the University of Maryland, and Egyptian fruit bats were imported from the Weizmann Institute of Science, Rehovot, Israel, both under permits from the Centers for Disease Control. Bats were housed under reversed 12-h light–dark conditions. *Carollia perspicillata* and *R. aegyptiacus* were maintained on a diet of fruits and water. *Eptesicus fuscus* were maintained on a diet of mealworms (*Tenebrio molitor*) and water. Husbandry and procedures were approved by the University of Maryland Institutional Animal Care and Use Committee and overseen by the United States Department of Agriculture.

Scanning electron microscopy.—Circular samples (13 mm diameter) at corresponding locations were taken from 26 different parts of the dorsal and ventral wings of 3 *E. fuscus*, 24 samples from the wings of 2 *C. perspicillata*, 28 samples from 2 *D. rotundus*, and 44 samples from 2 *R. aegyptiacus*. Samples fixed in 2.5% glutaraldehyde solution, washed in phosphate-buffered solution (PBS), and then fixed in 1% osmium tetroxide in PBS (60 min). After standard washing procedure with bi-distilled water, and dehydration in 75%, 95%, and 100% ethanol, the samples were dried in a critical point dryer (Denton DCP-1, Moorestown, New Jersey). The samples were mounted onto metal pedestals with silver paste, placed in a 50°C oven to harden, and then coated with gold palladium alloy (Denton DV-502/502 Vacuum Evaporator). The samples were viewed with a scanning electron microscope (Amray AMR-1610, Bedford, Massachusetts). Only intact and fully visible hairs were included in the taper measurements. Overall, 111 hairs from *E. fuscus*, 132 hairs from *C. perspicillata*, 118 hairs from *D. rotundus*, and 121 hairs from *R. aegyptiacus* were sampled. Wing membrane samples were collected from the dorsal and ventral propatagium, from different locations along the leading and trailing edge of the dactylopatagium, the membranes between the digits, and the medial portion and trailing edge of the plagiopatagium, the membrane between digit 5 (D5) and the body and leg in all 4 species, as well as the uropatagium in *R. aegyptiacus* and *E. fuscus*. The phyllostomid species (*D. rotundus* and *C. perspicillata*) have a very short tail, and consequently the uropatagium is reduced to a narrow band of membrane that could not be sampled with the required surface area.

Statistics.—All statistical tests were done with Origin (Pro) 2016. For comparisons of means, a 1-way ANOVA with Bonferroni correction for multiple comparisons and Levene test for equal variances were applied. $d.f. = 1$, $n − 1$ for all tests, because for each test, only 2 groups were compared. A simple linear regression was used to illustrate the relation between hair length and wing loading of each species.

RESULTS

Morphological parameters related to flight, e.g., body mass, wing span, wing aspect ratio, and wing loading, varied among the 4 species (Table 1). Although body mass and wingspan of *E. fuscus* and *C. perspicillata* were similar, *E. fuscus* exhibits an aspect ratio that is higher and a wing loading that is lower. Low body mass in combination with large wings is correlated with high maneuverability, as indicated by minimum turn angles (Norberg and Rayner 1987). The higher the aspect ratio, the longer and narrower is the wing; such a wing shape is typically found in fast-flying bats that hunt for insects in open space (Hayward and Davis 1964). Wing aspect ratio typically ranges from 5 to 14 in echolocating bats, and wing loading ranges from about 4.1 to 28 N/m², with large species having the highest loading values (Farney and Fleharty 1969; Lawlor 1973; Norberg 1994). Hence, *R. aegyptiacus* and also *D. rotundus* were close to the upper end of the wing loading spectrum, while *E. fuscus* and *C. perspicillata* were in the middle range.

Scanning electron microscopy.—In all 4 species, the scanning electron microscopy (SEM) analysis of the wing membranes revealed there were 2 populations of hairs on the wing: short, regularly distributed hairs (Fig. 1A), and up to several-millimeter-long pelage hair that is densely but irregularly distributed along the limbs, especially on the ventral side of the wing close to the body (Fig. 1B). In both *R. aegyptiacus* and *E. fuscus*, these pelage hairs also were found on the ventral and dorsal uropatagium. In contrast to the short hair, the pelage hair type was approximately 3 to 10 times longer, larger in diameter, and less tapered. The pelage hair typically had a spiny coronal or imbricate scale pattern and was easily distinguishable from the much smaller, tactile wing hair. In *C. perspicillata*, different

Table 1.—Body mass, wingspan, wing aspect ratio (wing span²/wing area), wing loading (body mass/wing area), and flight speed of the 4 bat species. *C.p.* = *Carollia perspicillata*; *D.r.* = *Desmodus rotundus*; *E.f.* = *Eptesicus fuscus*; *R.a.* = *Rousettus aegyptiacus*.

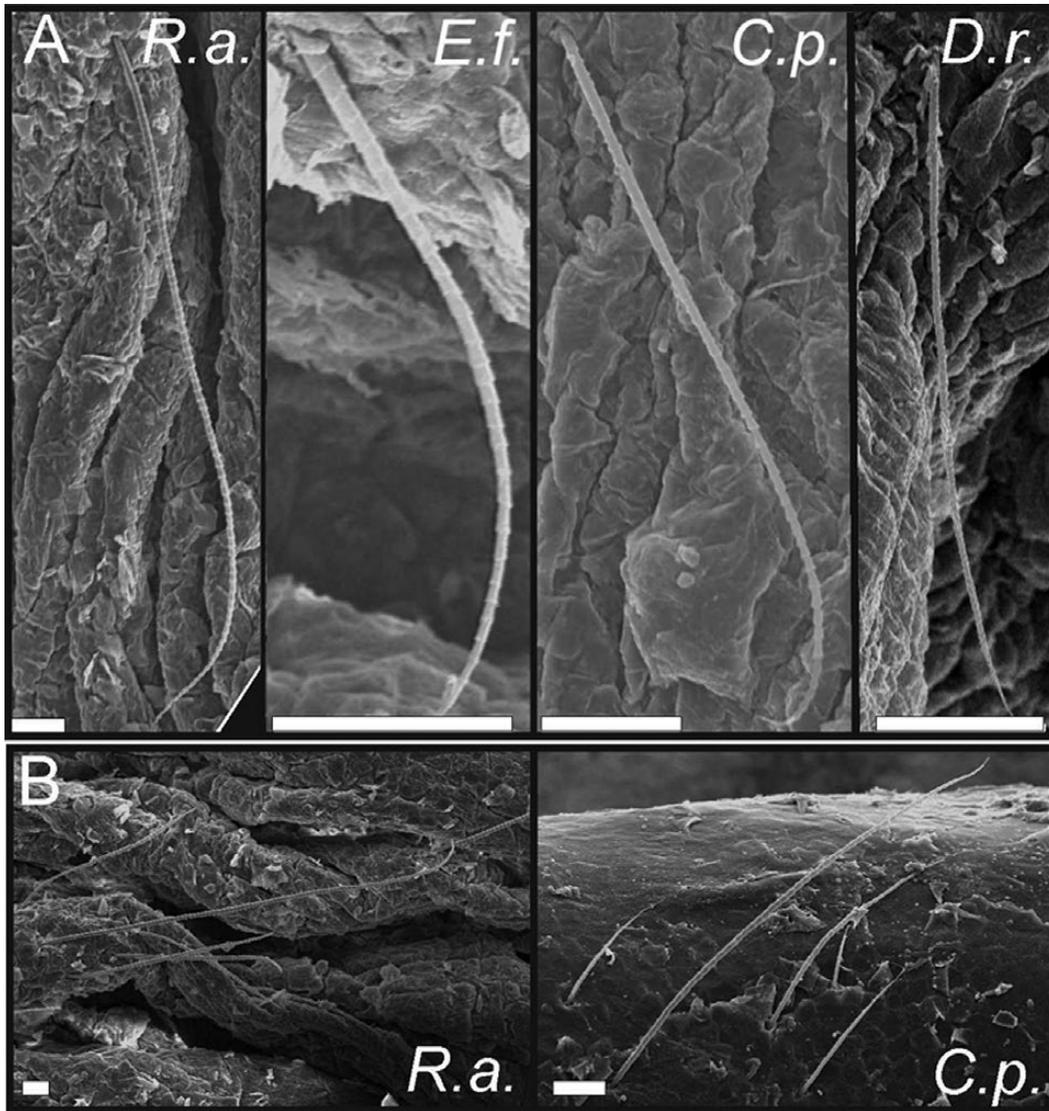| Species	Body mass (g)	Wing span (cm)	Aspect ratio	Wing loading (N/m²)	Flight speed (m/s)
E.f.	16	32	6.4	9.4	3.0–10
C.p.	19	32	6.1	11.4	2.0–4.5
D.r.	31	37	6.8	19.4	1.9–7.5
R.a.	140	57	5.9	24.6	3.0–8

Fig. 1.—Scanning electron microscope photomicrographs of wing hairs. A) Hairs from the dorsal dactylopatagium of the 4 species, from left: *Rousettus aegyptiacus* (*R.a.*), *Eptesicus fuscus* (*E.f.*), *Carollia perspicillata* (*C.p.*), and *Desmodus rotundus* (*D.r.*). B) Group of hairs on the dorsal dactylopatagium of *R.a.* and *C.p.* The white bars indicate 50 µm.

areas of the wing membrane were equipped with either single hairs, a mix of single hairs and small groups of 2–5 hairs (tufts), or only with grouped hairs.

Typically, hairs within groups were of different lengths. These groups were found on the dorsal and ventral wing surfaces except the dorsal wing tip and along most of the ventral trailing edge. In *R. aegyptiacus* and *D. rotundus*, groups or tufts of 2–7 hairs were found in similar areas as in *C. perspicillata*, but also in additional regions. Tufts of hairs were generally missing in *E. fuscus*, but 2 hairs protruding from 1 dome could be found occasionally on the dorsal and ventral plagiopatagium of this species (Fig. 2). These findings were consistent among all examined individuals of the same species.

Overall, 482 short hairs were analyzed, 132 in *C. perspicillata*, 111 in *E. fuscus*, 121 in *R. aegyptiacus*, and 118 in *D. rotundus.* The regularly distributed short hairs were strongly tapered, only a few micrometers thick at the base (means ± *SD*: *E. fuscus*: 4.59 ± 0.94 µm; *C. perspicillata*: 5.03 ± 1.03 µm; *R. aegyptiacus*: 11.04 ± 3.31 µm; *D. rotundus*: 7.85 ± 2.66 µm). The hairs ended in a thin wisp that was less than 1 µm in diameter in the 3 laryngeal echolocators (means: *E. fuscus*: 0.8 µm; *C. perspicillata*: 0.63 µm; *D. rotundus*: 0.72 µm), but in a more blunt tip of 4.68 µm in *R. aegyptiacus*. Often, but not always, these hairs were found along the elastin bands that run through the wing membrane (Fig. 3A). The hairs also could be found in membrane regions away from elastin bands, over bone structures, as well as a "fringe" at the very edge of the membrane (Fig. 3B) in all species. Each hair scale consisted of only a single follicle cell resulting in a simple, smooth coronal pattern (Debelica and Thies 2009). The average density of the wing membrane hairs was low with about 1–3 hairs/mm^2 membrane surface on the dactylopatagium and plagiopatagium in all species, but could be considerably higher in some areas close to the arm on the propatagium of the larger *R. aegyptiacus* and *D. rotundus*.
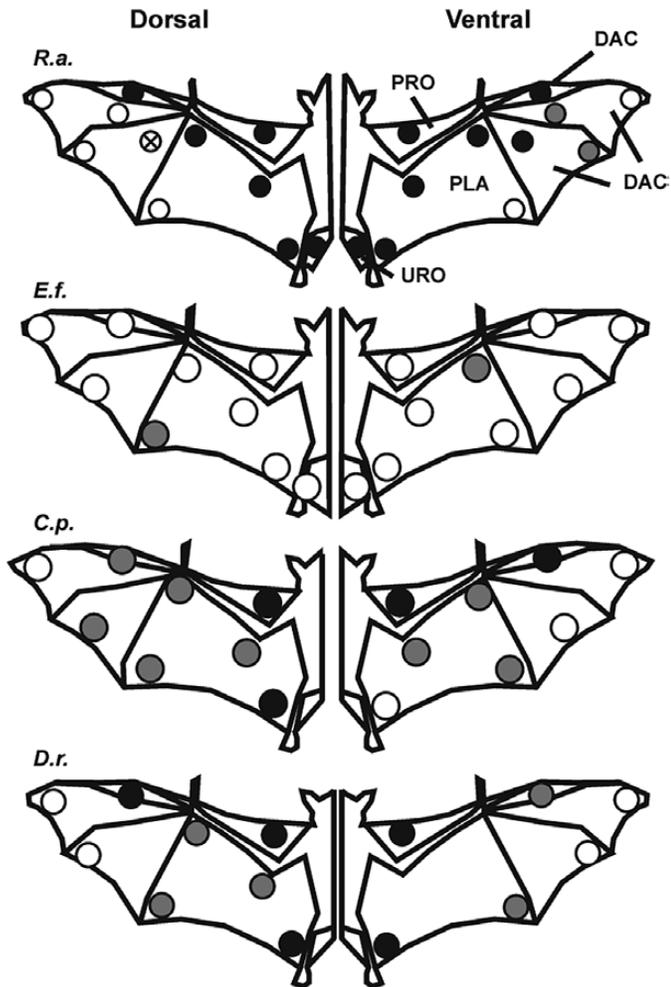
Fig. 2.——Locations of wing membrane samples collected from 4 species of bats, from top: *Rousettus aegyptiacus* (*R.a.*), *Eptesicus fuscus* (*E.f.*), *Carollia perspicillata* (*C.p.*), and *Desmodus rotundus* (*D.r.*). Dorsal locations are shown on the left, ventral locations on the right. Open circles mark locations, where only single hairs were found, gray colored circles mark locations that had a mix of single hairs and grouped hairs. Black colored circles indicate locations with mostly groups. The locations marked in gray in *E.f.* contained a mix of pairs of hairs and single hairs, and no larger groups. The dorsal location marked with an X in *R.a.* did not have any hairs in both specimens. DAC = dactylopatagium; PLA = plagiopatagium; PRO = propatagium; URO = uropatagium.

Hair density tended to be lower along the trailing edges of the wings examined for 3 of the 4 bat species, but not in *C. perspicillata*. It did not differ significantly between the leading and trailing edge samples in *R. aegyptiacus* and *D. rotundus* (Fig. 4A). All 4 species showed significant decreases in hair length between leading edge (propatagium and rostral dactylopatagium including wing tip) and trailing edge (caudal plagiopatagium and dactylopatagium) locations (Fig. 4B). Hair length correlated well with the wing loading value of each species for both the leading and trailing edge (Fig. 4C). The regressions between hair length and wing aspect ratio or flight speed were not significant. Also, diet—and therefore the foraging behavior each diet requires—did not regress significantly with hair length.
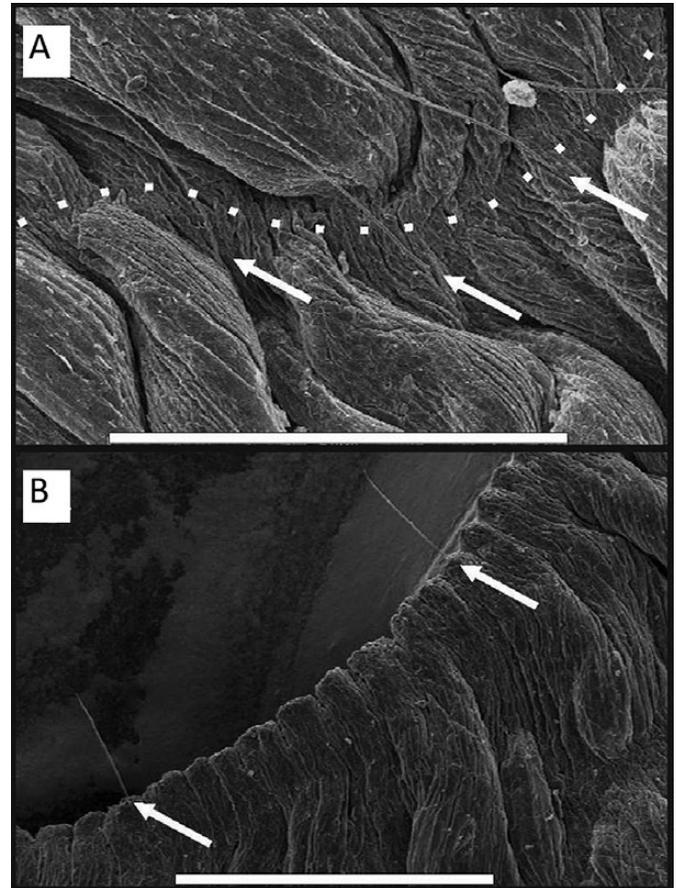

Fig. 3.—A) Hairs, marked with arrows, next to an elastin band (dotted line) on the dorsal plagiopatagium of *Desmodus rotundus*. B) Hairs on the very caudal edge of the dactylopatagium of *D. rotundus*. The white bars indicate 1 mm.

The distributions of hair tip and base diameters from all hairs (entire dorsal and ventral surface), which varied among the 4 species, are illustrated in Fig. 5A. Hair taper, as a percentage of hair length, revealed that *R. aegyptiacus* hairs are the least tapered (Fig. 5B). However, mean taper of the closely related phyllostomids *C. perspicillata* and *D. rotundus* was not statistically different, although these species do differed significantly with respect to hair base diameter, body size (Table 1), and diet. The largest statistical differences for base diameter, tip diameter, and taper occur between *R. aegyptiacus* (Yangochiroptera) and the 3 laryngeal echolocators (Yinpterochiroptera).

Discussion

We found 2 distinct types of hairs on the bat wing: a longer pelage hair that is found close to the body of the animal and a very short, strongly tapered type of hair that is found on almost all membranous parts of the wing, including the ventral wing surface. Finding hairs on the ventral dactylopatagium in all 4 species is of particular interest, because in other mammals the ventral side of the hand is glabrous, hence free of hair. This finding indicates that the processes during embryological development of the dactylopatagium that derives from
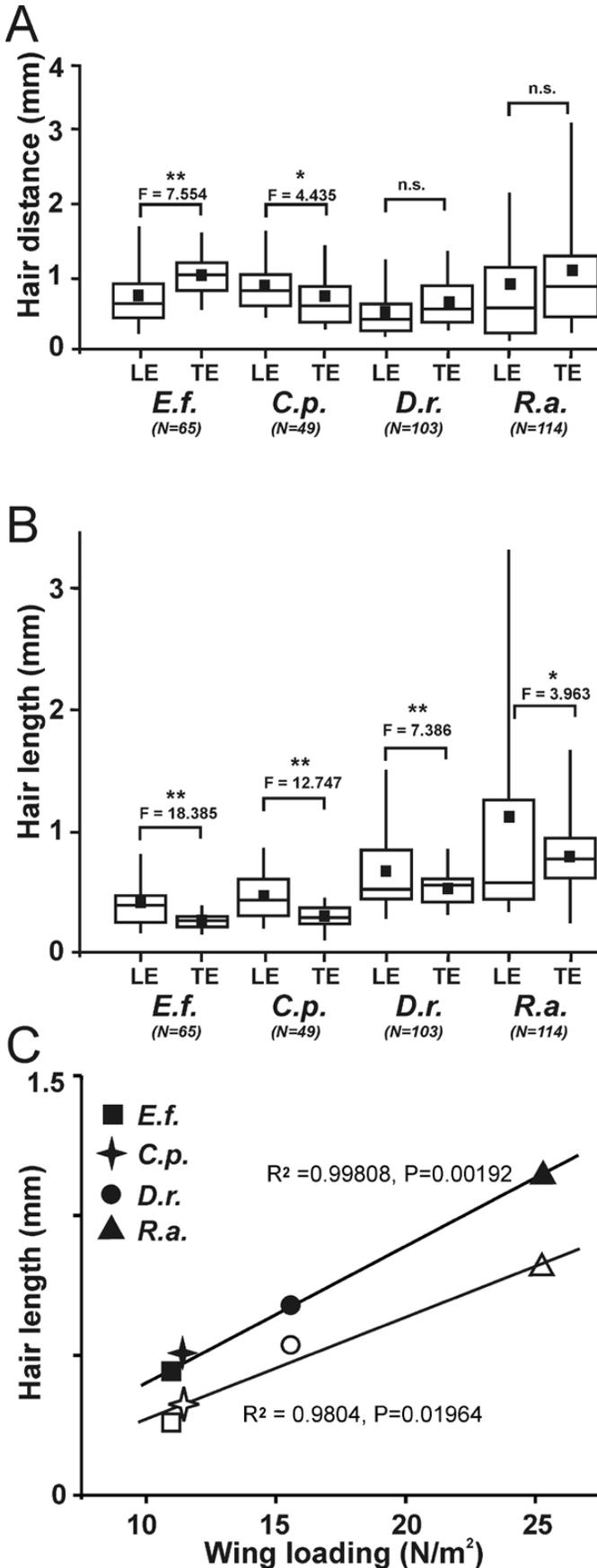
embryonal interdigital webbing that is not subject to apoptosis in bats (Weatherbee et al. 2006) also promote hair growth. The inhibition of bone morphogenetic protein signaling which plays a role during early skeletal formation triggers ectopic hair development on glabrous skin in mice. Therefore, the anti-apoptotic mechanisms that govern wing membrane formation in bats might also account for the unusual expansion of hair follicles on the ventral surface as an evolutionary adaptation for sensing airflow (Mayer et al. 2008). Furthermore, the hairs found on the plagiopatagium, which grows out of the flank of the embryo and ultimately attaches to digit 5 (Cretekos et al. 2005), do not differ morphologically from hairs found on the dactylopatagium.

The pelage hair type does not protrude from a dome-like structure like the short hairs found on the wing. According to Bullen and McKenzie (2008), these long hairs might smooth the contour of the bat in wing regions that have sharp angles, e.g., close to the trunk, arms, and legs, and therefore passively improve aerodynamics of the flying bat by reducing drag. The short hairs are so sparsely distributed that viscous coupling between single hairs can be excluded (Lewin and Hallam 2010), unless the hairs protrude from the same dome, such as the groups or tufts of hairs that we found frequently in 3 of the 4 species we studied. In any case, the distance between the groups or tufts is similar to the distance between single hairs, and therefore large enough to avoid viscous coupling between the groups that might function collectively as sensory units. Preliminary data suggest that hair groups or tufts may share the receptor substrate of the dome (Sterbing-D'Angelo and Moss 2014). Further investigations are needed to confirm this observation. The only insectivorous vespertilionid species included in this study did not show significant grouping of hairs, whereas the phyllostomids and the Egyptian fruit bat had grouped or tufted hairs over a large wing area. It is noteworthy that a larger, insectivorous vespertilionid bat, the pallid bat, *Antrozous pallidus* (20–35 g), also shows groups of hairs protruding from single domes (Zook and Fowler 1986). These facts suggest that neither body mass nor phylogenetic affinity seem to be a factor.

Functionally, the short length of the bat wing hairs makes them suitable for responding to boundary layer flow, close to the membrane surface where air is viscous (Dickinson 2010). A sharp taper has functional implications: it assures that the

Fig. 4.—A) Mean distance between hairs compared for leading edge (LE) versus trailing edge (TE) of the bat wing of the 4 species, from left: *Eptesicus fuscus* (*E.f.*), *Carollia perspicillata* (*C.p.*), *Desmodus rotundus* (*D.r.*), and *Rousettus aegyptiacus* (*R.a.*). Mean (solid squares), median (horizontal line in box), interquartile range (box), and 5th and 95th percentiles (whiskers) are shown. Groups that are significantly different at the 0.05 level are indicated with "*", and those that differ at the 0.01 level with "**". B) Mean length of the hairs on LE and TE wing regions. Graph organization same as (A). C) Leading edge (solid symbols) and trailing edge (open symbols) hair length plotted versus wing loading of the 4 bat species. For both the LE and TE, hair length is related to wing loading (linear regression, R^2 and P values next to regression lines).
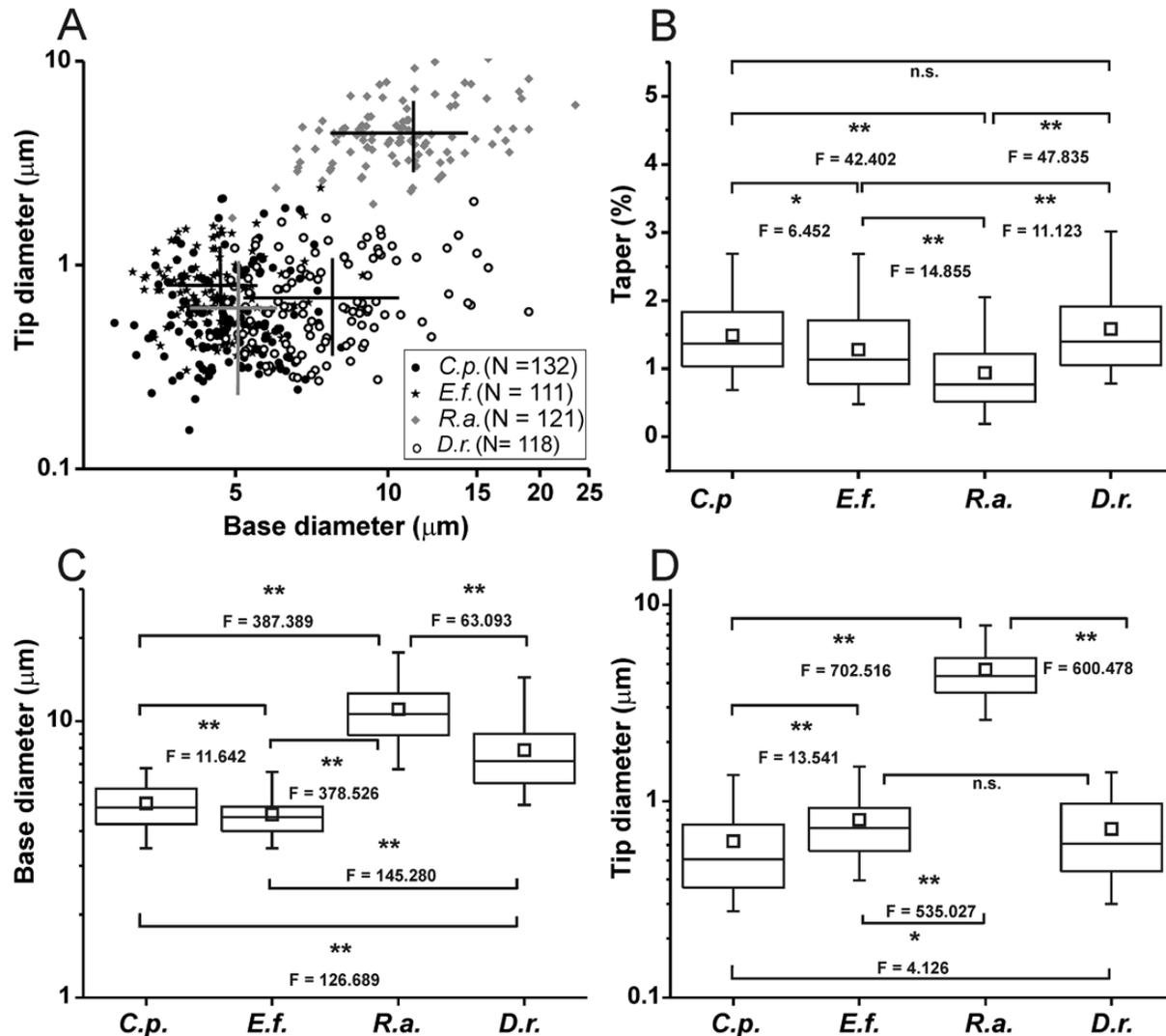
Fig. 5.—Morphological parameters of wing hairs in 4 bat species, from left: *Carollia perspicillata* (*C.p.*), *Eptesicus fuscus* (*E.f.*), *Rousettus aegyptiacus* (*R.a.*), and *Desmodus rotundus* (*D.r.*). A) Log base and tip diameter of the hairs in micrometer. The bars indicate *SD* for tip and base diameter. B) Mean (open squares), median (horizontal line in box), interquartile range (box), and 5th and 95th percentiles (whisker) of the hair taper in % across species are shown. C) Same statistical measures for the hair base diameter and D) for the hair tip diameter. Groups that are significantly different at the 0.05 level are indicated with "*", and those that differ at the 0.01 level with "**".

breakage point of the hair is very close to the tip. Consequently, mass of the hair does not change appreciably when breakage occurs (Williams and Kramer 2010). Dickinson's (2010) modeling results suggest that linearly tapered hairs provide greater output sensitivity than hairs of uniform cross-section. Dickinson (2010) concluded that computed optimal hair lengths are in agreement with the range of hair lengths found in *E. fuscus*, *Glossophaga soricina*, and *Pteropus poliocephalus*. These modeling results support the hypothesis that bats use tactile hairs to detect changes in boundary layer shape (Dickinson 2010). We further suggest that hairs within multi-hair tufts that typically have different lengths are well suited to monitor shear in different sublayers of the boundary layer flow, i.e., in the viscous and the buffer layer at the same location. Common to all 4 bat species in the present study is the finding that microscopic tactile hairs are significantly shorter close to the trailing edge of the wing. Also, they are stiffer than hairs at the leading

edge of the wing (Sterbing-D'Angelo et al. 2016). This finding suggests that it may be advantageous to limit hair length to fall within the airflow sublayers along the trailing edge (e.g., viscous layer, buffer layer, turbulent layer). In general, hair length is related to body mass and wing loading values across species, i.e., larger species had longer hairs. This is expected, because thickness of the boundary layer depends on the Reynolds number, the product of airflow velocity and chord length divided by the kinetic viscosity of air. Hence, at a given flow velocity and viscosity, the Reynolds number increases with the rostro-caudal (chord) length of the wing.

We frequently observed broken tips in bat wing hairs in the SEM analysis, and as predicted by the taper, breaks were always found at one of the most distal segments. This breakage has a negligible effect on a hair's mass. A hair was classified as intact by the species-specific tip diameter and, most importantly, by the shape of the last segment that is elongated in intact

hair. Only fully intact hairs were included for the taper measurements in this study, and it is unclear whether the observed breaks occurred before or after tissue preparation for the SEM.

In summary, we show that sparse grids of short tactile wing hairs are ubiquitous in a variety of bat species, and their anatomy and distribution across the wing membrane show little variation, in spite of the very different embryonic origins of wing membrane segments and flight and diet specializations of the 4 species studied. The dimensions of the hairs correlate with wing loading and body mass of each species, but not with wing aspect ratio, flight speed, or diet and lifestyle. In all species, hairs located along the trailing edge are significantly shorter than those on the leading edge of the wing on both the dorsal and ventral surfaces. The length of wing hairs appears to scale to average boundary layer thickness of each bat species, which depends on airfoil dimensions and Reynolds number.

ACKNOWLEDGMENTS

LITERATURE CITED

BULLEN, R. D., AND N. L. MCKENZIE. 2008. Aerodynamic cleanliness in bats. Australian Journal of Zoology 56:281–296.

CRETEKOS, C. J., ET AL. 2005. Embryonic staging system for the short-tailed fruit bat, *Carollia perspicillata*, a model organism for the mammalian order Chiroptera, based upon timed pregnancies in captive-bred animals. Developmental Dynamics 233:721–738.

DEBELICA, A., AND M. L. THIES. 2009. Atlas and key to the hair of terrestrial Texas mammals. Pp. 1–102 in Special publications of the Museum of Texas Tech University, Number 55 (R. J. Baker, ed.). Museum of Texas Tech University Press, Lubbock.

DICKINSON, B. T. 2010. Hair receptor sensitivity to changes in laminar boundary layer shape. Bioinspiration & Biomimetics 5:16002.

FARNEY, J., AND E. D. FLEHARTY. 1969. Aspect ratio, loading, wing span, and membrane areas of bats. Journal of Mammalogy 50:362–367.

HAYWARD, B., AND R. DAVIS. 1964. Flight speeds in western bats. Journal of Mammalogy 45:236–242.

LAWLOR, T. E. 1973. Aerodynamic characteristics of some Neotropical bats. Journal of Mammalogy 54:71–78.

LEWIN, G. C., AND J. HALLAM. 2010. A computational fluid dynamics model of viscous coupling of hairs. Journal of Comparative Physiology, A: Neuroethology, Sensory, Neural, and Behavioral Physiology 196:385–395.

MAYER, J. A., J. FOLEY, D. DE LA CRUZ, C. M. CHUONG, AND R. WIDELITZ. 2008. Conversion of the nipple to hair-bearing epithelia by lowering bone morphogenetic protein pathway activity at the dermal-epidermal interface. The American Journal of Pathology 173:1339–1348.

MUIJRES, F. T., L. CHRISTOFFER JOHANSSON, Y. WINTER, AND A. HEDENSTRÖM. 2014. Leading edge vortices in lesser long-nosed bats occurring at slow but not fast flight speeds. Bioinspiration & Biomimetics 9:025006.

MUIJRES, F. T., L. C. JOHANSSON, R. BARFIELD, M. WOLF, G. R. SPEDDING, AND A. HEDENSTRÖM. 2008. Leading-edge vortex improves lift in slow-flying bats. Science 319:1250–1253.

NORBERG, U. 1994. Wing design, flight performance, and habitat use in bats. Pp. 205 in Ecological morphology (P. C. Wainwright and S. M. Reilly, eds.). The University of Chicago Press Ltd, Chicago, IL.

NORBERG, U. M., AND J. M. RAYNER. 1987. Ecological morphology and flight in bats (Mammalia; Chiroptera): wing adaptations, flight performance, foraging strategy and echolocation. Philosophical Transactions of the Royal Society B: Biological Sciences 316:335–427.

SIKES, R. S. AND ANIMAL CARE AND USE COMMITTEE OF THE AMERICAN SOCIETY OF MAMMALOGISTS. 2016. Guidelines of the American Society of Mammalogists for the use of wild mammals in research and education. Journal of Mammalogy 97:663–688.

STERBING-D'ANGELO, S., ET AL. 2011. Bat wing sensors support flight control. Proceedings of the National Academy of Sciences 108:11291–11296.

STERBING-D'ANGELO, S. J., M. CHADHA, K. L. MARSHALL, AND C. F. MOSS. 2017. Functional role of airflow-sensing hairs on the bat wing. Journal of Neurophysiology 117:705–712.

STERBING-D'ANGELO, S. J., AND MOSS, C. F. 2014. Air flow sensing in bats. Pp. 197–213 in Flow sensing in air and water – behavioral, neural and engineering principles of operation (H. Bleckmann, J. Mogdans, and S. L. Coombs, eds.) Springer, Heidelberg, Germany.

STERBING-D'ANGELO, S. J., H. LIU, M. YU, AND C. F. MOSS. 2016. Morphology and deflection properties of bat wing sensory hairs: scanning electron microscopy, laser scanning vibrometry, and mechanics model. Bioinspiration & Biomimetics 11:056008.

WEATHERBEE, S. D., R. R. BEHRINGER, J. J. RASWEILER, AND L. A. NISWANDER. 2006. Interdigital webbing retention in bat wings illustrates genetic changes underlying amniote limb diversification. Proceedings of the National Academy of Sciences 103:15103–15107.

WILLIAMS, C. M., AND E. M. KRAMER. 2010. The advantages of a tapered whisker. PLoS one 5:e8806.

ZOOK, J. M., AND B. C. FOWLER. 1986. A specialized mechanosensory array of the bat wing. Myotis 23–24:31–36.